

Critical fields and the spontaneous vortex state in the weakly ferromagnetic superconductor $\text{RuSr}_2\text{GdCu}_2\text{O}_8$

C. Y. Yang, B. C. Chang, and H. C. Ku*

Department of Physics, National Tsing Hua University, Hsinchu, Taiwan 300, Republic of China

Y. Y. Hsu

Institute of Physics, Academia Sinica, Taipei, Taiwan 115, Republic of China

(Received 30 June 2005; published 15 November 2005)

A spontaneous vortex state (SVS) between 30 and 56 K was observed for the weak-ferromagnetic superconductor $\text{RuSr}_2\text{GdCu}_2\text{O}_8$ with the ferromagnetic Curie temperature $T_C=131$ K and the superconducting transition temperature $T_c=56$ K. The low-field (± 20 G) superconducting hysteresis loop indicates a narrow Meissner state region within the average lower critical field $B_{c1}(T)=B_{c1}(0)[1-(T/T_0)^2]$, with average $B_{c1}^{\text{ave}}(0)=12$ G and $T_0=30$ K. Full Meissner shielding signal in very low applied field indicates an *ab* plane $B_{c1}^{ab}(0)\sim 4$ G with an estimated anisotropic parameter $\gamma\sim 7$ for this layered system. The existence of a spontaneous vortex state between 30 and 56 K is the result of weak-ferromagnetic order with a net spontaneous magnetic moment of $\sim 0.1\mu_B/\text{Ru}$, which generates a weak magnetic dipole field around 10 G in the CuO_2 bilayers. The upper critical field B_{c2} varies linearly as $(1-T/T_c)$ up to 7-T field. The vortex melting line B_m varies as $(1-T/T_m)^{3.5}$ with melting transition temperature $T_m=39$ K and a very broad vortex liquid region due to the coexistence and the interplay between superconductivity and weak-ferromagnetic order.

DOI: [10.1103/PhysRevB.72.174508](https://doi.org/10.1103/PhysRevB.72.174508)

PACS number(s): 74.72.-h, 74.25.Ha

I. INTRODUCTION

Recently, high- T_c superconductivity with anomalous magnetic properties was reported in the weak-ferromagnetic Ru-1212 system $\text{RuSr}_2\text{RCu}_2\text{O}_8$ ($R=\text{Sm, Eu, Gd, Y}$) with the tetragonal $\text{TiBa}_2\text{CaCu}_2\text{O}_7$ -type structure.¹⁻⁴³ For the Ca-substituted system, a possible superconductivity was also reported in the weak-ferromagnetic compounds $\text{RuCa}_2\text{RCu}_2\text{O}_8$ ($R=\text{Pr-Gd}$).⁴⁴⁻⁴⁶ The metallic weak-ferromagnetic (WFM) order is originated from the long-range order of Ru moments in the RuO_6 octahedra due to strong $\text{Ru-}4d_{xy,yz,zx}\text{-O-}2p_{x,y,z}$ hybridization in this strongly correlated electron system. The Curie temperature $T_C\sim 130$ K observed from magnetization measurement in the prototype compound $\text{RuSr}_2\text{GdCu}_2\text{O}_8$ is probably a canted *G*-type antiferromagnetic order with Ru^{5+} moment μ canted along the tetragonal basal plane resulting a small net spontaneous magnetic moment $\mu_s\ll\mu(\text{Ru}^{5+})$ too small to be detected in neutron diffraction.^{4,5,9,10,21} The occurrence of high- T_c superconductivity with maximum resistivity onset $T_c(\text{onset})\sim 60$ K in $\text{RuSr}_2\text{GdCu}_2\text{O}_8$ is related with the quasi-two-dimensional CuO_2 bilayers separated by a rare-earth layer in the Ru-1212 structure.^{1,2,4,5,29} Broad resistivity transition width $\Delta T_c=T_c(\text{onset})-T_c(\text{zero})\sim 15\text{--}20$ K observed is most likely originated from the coexistence and the interplay between superconductivity and weak-ferromagnetic order.¹⁻⁴³ The diamagnetic T_c is observed anomalously at lower temperature near $T_c(\text{zero})$ instead of at $T_c(\text{onset})$, and a reasonably large Meissner signal was reported using stationary sample magnetometer with diamagnetic $T_c\sim 30$ K in ≤ 1 G applied field at zero-field-cooled (ZFC) mode.³⁸ Lower $T_c(\text{onset})\sim 40$ and 12 K were observed for $\text{RuSr}_2\text{EuCu}_2\text{O}_8$ and $\text{RuSr}_2\text{SmCu}_2\text{O}_8$, respectively.^{12,17} No superconductivity can be detected in $\text{RuSr}_2\text{RCu}_2\text{O}_8$

($R=\text{Pr, Nd}$).^{3,16} Superconducting $\text{RuSr}_2\text{YCu}_2\text{O}_8$ phase is stable only under the high pressure.^{20,25} The physics is still unclear in this system, and it will be interesting to investigate the effect of the weak-ferromagnetic order on the superconducting critical fields B_{c2} and B_{c1} , as well as on the possible existence of a spontaneous vortex state (SVS) at a higher temperature above the Meissner state.

II. EXPERIMENTAL

The stoichiometric $\text{RuSr}_2\text{GdCu}_2\text{O}_8$ samples were synthesized by the standard solid-state reaction method. High-purity RuO_2 (99.99 %), SrCO_3 (99.99 %), Gd_2O_3 (99.99 %), and CuO (99.99 %) preheated powders with the nominal composition ratio of $\text{Ru}:\text{Sr}:\text{Gd}:\text{Cu}=1:2:1:2$ were well mixed and calcined at 960°C in air for 16 h. The calcined powders were then pressed into pellets and sintered in flowing N_2 gas at 1015°C for 10 h to form $\text{RuSr}_2\text{GdO}_6$ and Cu_2O precursors. This step is crucial in order to avoid the formation of unwanted impurity phases. The N_2 -sintered pellets were heated at 1060°C in flowing O_2 gas for 10 h to form the Ru-1212 phase. The pellets were oxygen annealed at slightly higher 1065°C for 5 days and slowly furnace cooled to room temperature with a rate of 15°C per h .¹⁵

The powder x-ray diffraction data were collected with a Rigaku Rotaflex 18-kW rotating anode diffractometer using graphite monochromatized $\text{Cu-K}\alpha$ radiation with a scanning step of 0.02° (10 s counting time per step) in the 2θ ranges of $5^\circ\text{--}100^\circ$. The electrical resistivity and magnetoresistivity measurements were performed using the standard four-probe method with a Linear Research LR-700 ac (16Hz) resistance bridge from 2 to 300 K with applied magnetic field up to 7 T. The magnetization, magnetic susceptibility, and magnetic hysteresis measurements from 2 to 300 K with applied fields

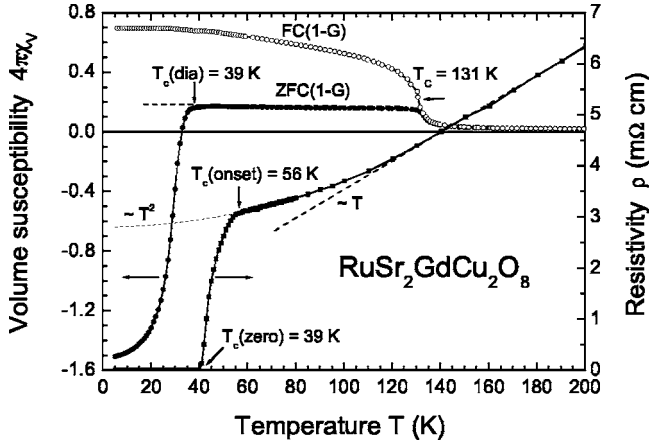


FIG. 1. Electrical resistivity $\rho(T)$ and volume magnetic susceptibility $\chi_V(T)$ at 1-G field-cooled (FC) and zero-field-cooled (ZFC) modes for oxygen-annealed $\text{RuSr}_2\text{GdCu}_2\text{O}_8$.

from 1 G to 7 T were carried out with a Quantum Design 1-T μ -metal shielded MPMS2 or a 7-T MPMS superconducting quantum interference device (SQUID) magnetometer.

III. RESULTS AND DISCUSSION

The powder x-ray diffraction pattern for the oxygen-annealed $\text{RuSr}_2\text{GdCu}_2\text{O}_8$ polycrystalline sample indicates close to a single phase with the tetragonal lattice parameters of $a=0.5428(5)\text{nm}$ and $c=1.1589(9)\text{nm}$. The space group $P4/mbm$ is used for Rietveld refinement analysis, where neutron-diffraction data indicate that a RuO_6 octahedra 14° rotation around the c axis is needed to accommodate physically reasonable Ru-O bond lengths.¹⁰ The refinement with the fixed 14° rotation angle gives a good residual error R of 3.64%, weighted pattern error $R_{\text{WP}}=6.07\%$, and Bragg error $R_B=5.05\%$.

The temperature dependence of the electrical resistivity $\rho(T)$ and the volume magnetic susceptibility $\chi_V(T)$ at 1-G field-cooled (FC) and zero-field-cooled (ZFC) modes for $\text{RuSr}_2\text{GdCu}_2\text{O}_8$ are shown collectively in Fig. 1. The high-temperature resistivity decreases monotonically from room temperature value of 9.2 mΩ cm (not shown) to 6.4 mΩ cm at 200 K, and extrapolated to 2.8 mΩ cm at 0 K with a good resistivity ratio $\rho(300\text{ K})/\rho(0\text{ K})$ of 3.3 for the polycrystalline sample. The high-temperature resistivity shows a non-Fermi-liquid-like linear T dependence down to a Curie temperature T_C of 131 K, then changes to a T^2 behavior below T_C due to magnetic order.

The superconducting onset temperature of 56 K is determined from the deviation from T^2 behavior, with a zero resistivity $T_{c(\text{zero})}$ at 39 K. The broad transition width $\Delta T_C=17\text{ K}$ observed is the common feature for all reported Ru-1212 resistivity data, which indicates that the superconducting Josephson coupling along the tetragonal c axis between Cu-O bilayers may be partially blocked by the dipole field B_{dipole} of ordered Ru moments in the Ru-O layer.^{1,2,4,5,29,40} The diamagnetic T_c at 39 K was observed in the 1-G ZFC susceptibility measurement. The full Meissner

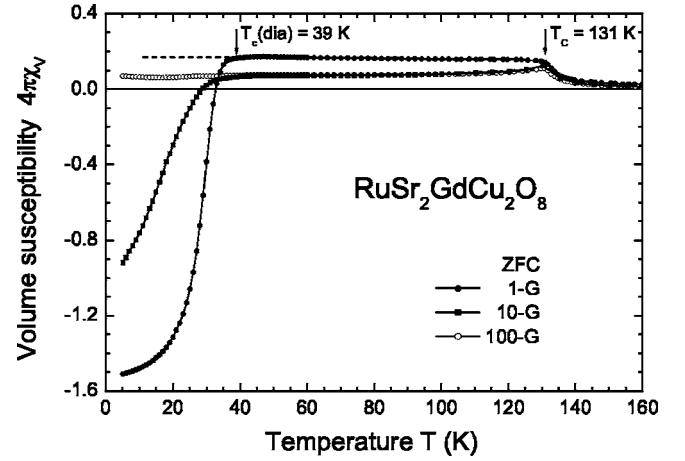


FIG. 2. ZFC volume susceptibility $\chi_V(T)$ for $\text{RuSr}_2\text{GdCu}_2\text{O}_8$ at 1, 10, and 100 G. Note that the full Meissner shielding signal was observed only at low applied field and low temperature.

shielding signal $4\pi\chi_V=4\pi M/B_a \sim -1.5$ (Gaussian units) was recorded at 5 K. This value is identical to the Meissner shielding signal expected for a superconducting sphere with a demagnetization factor N of $-4\pi/3$ and in an applied field B_a well below lower critical field B_{c1} . The large diamagnetic signal in 1-G ZFC mode is the best data observed so far from various reported susceptibility measurement techniques.^{4,5,28,29,38} Since our measurements were performed with the standard moving-sample SQUID magnetometer, it is clear that sample quality is more crucial than measuring techniques. Both ZFC and FC data reveal a Curie temperature T_C of 131 K. However, in 1-G FC mode, no diamagnetic field-expulsion signal can be detected below 39 K due to strong flux pinning where superconductivity coexists with weak-ferromagnetic order.

The zero-field-cooled (ZFC) volume susceptibility $\chi_V(T)$ at 1, 10, and 100 G applied fields are shown collectively in Fig. 2. All data show the same magnetic order $T_C(\text{Ru})$ of 131 K. Although the diamagnetic T_c of 39 K was still observed at 10-G ZFC measurement, the diamagnetic signal at 5 K is reduced to 60% of the full Meissner signal. Consider the polycrystalline nature of sample with varying microcrystallite size and orientation, the average superconducting lower critical field B_{c1} at 5 K is estimated to be close to 10 G. No net diamagnetic signal can be detected at 100-G ZFC mode where the sample is already in the vortex glass or lattice state and the small diamagnetic signal is overshadowed by a large weak-ferromagnetic background.³⁸

Based on this information, the low-field ($\pm 20\text{ G}$) isothermal superconducting hysteresis loops $M-B_a$ are measured and collectively shown in Figs. 3(a) (5, 10, 15, and 20 K) and 3(b) (25, 30, and 35 K). The initial magnetization curve deviates from straight line in 4 G at 5 K, 3.5 G at 10 K, 3 G at 15 K, 2 G at 20 K, and 1 G at 25 K. This is the narrow region that full Meissner signals are detected and is roughly corresponding to the anisotropic lower critical field in the ab plane $B_{c1}^{ab}(T)$ with $B_{c1}^{ab}(0) \sim 4\text{ G}$. The average lower critical field B_{c1}^{ave} for the polycrystalline sample is determined from

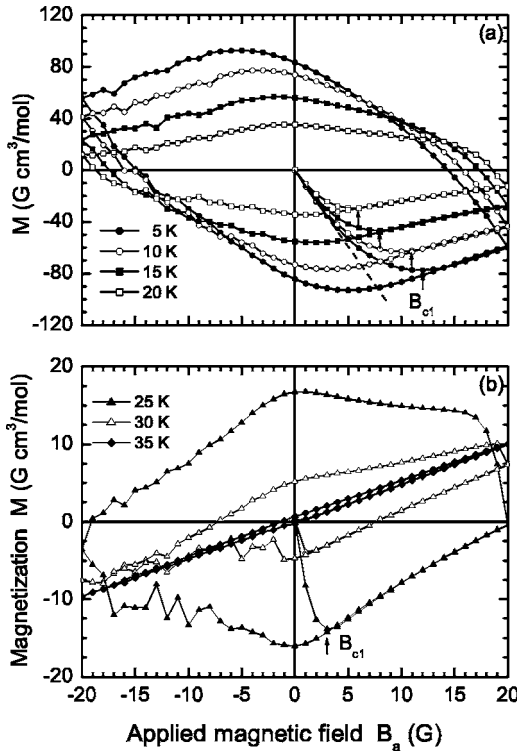


FIG. 3. Low-field superconducting hysteresis loops M - B_a for $\text{RuSr}_2\text{GdCu}_2\text{O}_8$: (a) at 5, 10, 15, 20 K and (b) at 25, 30, and 35 K.

the peaks of initial diamagnetic magnetization curves. The effect on the exact peak value due to the surface barrier pinning is neglected. B_{c1} decreases steadily from 12 G at 5 K, 11 G at 10 K, 9 G at 15 K, 6 G at 20 K, 3 G at 25 K, and below 1 G at 30 K. A simple empirical parabolic fitting gives $B_{c1}(T) = B_{c1}(0)[1 - (T/T_0)^2]$, with average $B_{c1}^{\text{ave}}(0) = 12$ G and $T_0 = 30$ K (see Fig. 4). Using the anisotropic Ginzburg-Landau formula $B_{c1}^{\text{ave}} = [2B_{c1}^{\text{ab}} + B_{c1}^c]/3$, c -axis $B_{c1}^c \sim 28$ G and the anisotropy parameter $\gamma \sim 7$ is estimated. This value is close to a reported anisotropy γ value for

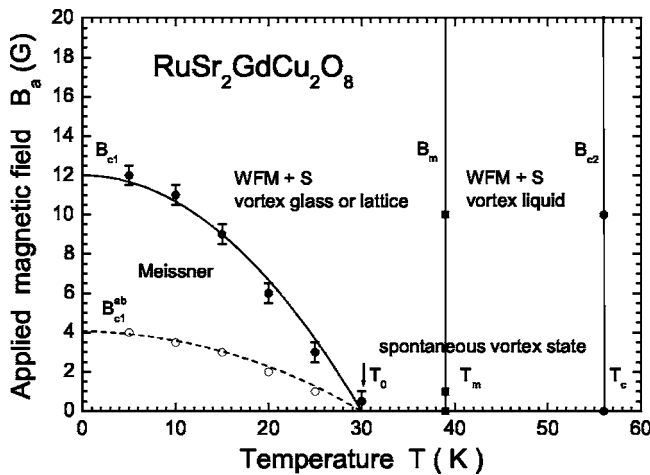


FIG. 4. The lower field, low-temperature superconducting phase diagram $B_a(T)$ of $\text{RuSr}_2\text{GdCu}_2\text{O}_8$.

$\text{YBa}_2\text{Cu}_3\text{O}_7$ where the 123-type structure can be written as $\text{Cu-1212 CuBa}_2\text{YCu}_2\text{O}_7$. An average penetration depth $\lambda_{\text{ave}}(0) = [\Phi_0/2\pi B_{c1}^{\text{ave}}(0)]^{1/2}$ of 520 nm was derived with estimated $\lambda_{ab}(0) = 340$ nm and $\lambda_c(0) = 2400$ nm from $B_{c1}^c = \Phi_0/2\pi\lambda_{ab}^2$ and $B_{c1}^{\text{ab}} = \Phi_0/2\pi\lambda_{ab}\lambda_c$, where Φ_0 is flux quantum.

Since $T_0 = 30$ K is well below $T_c(\text{onset}) = 56$ K and $T_c(0) = 39$ K in zero applied field, a spontaneous vortex state (SVS) indeed exists between 30 and 56 K. The low-field phase diagram $B_a(T)$ for the polycrystalline sample is shown in Fig. 4, with the average $B_{c1}(T)$ separates the Meissner state from the vortex state and a smaller $B_{c1}^{\text{ab}}(T)$ inside the Meissner region for reference. $T_c(0) = 39$ K in the broad resistive transition is the onset of vortex depinning by a driving current. This temperature is very close to the melting transition temperature T_m from the spontaneous vortex glass or lattice state to the spontaneous liquid state due to nonzero dipole field B_{dipole} of weak-ferromagnetic order. The upper critical field B_{c2} defined from $T_c(\text{onset})$ and the vortex melting field $B_m(T)$ defined from $T_c(0)$ are temperature independent for small applied fields below 20 G. The internal dipole field generated by a weak-ferromagnetic order can be estimated using a simple extrapolation $[B_{c1}(0) + B_{\text{dip}}]/B_{c1}(0) = T_c/T_0 = 56 \text{ K}/30 \text{ K}$, which results with a dipole field $B_{\text{dipole}} \sim 10.4$ G on the CuO_2 bilayers. A small net spontaneous magnetic moment μ_s of $\sim 0.11\mu_B$ per Ru is estimated using $B_{\text{dipole}} \sim 2\mu_s/d^3$ with $d = c/2 = 0.58$ nm which is the distance between midpoint of CuO_2 bilayers and two nearest-neighbor Ru moments. If the weak-ferromagnetic structure is a canted G -type antiferromagnetic order with Ru moments $\mu (=1.5\mu_B$ for Ru^{5+} in t_{2g} states) canted along the tetragonal basal plane, the small net spontaneous magnetic moment gives a canting angle of 4° from the tetragonal c axis and is difficult to be detected in neutron diffraction with a resolution around $0.1\mu_B$.^{9,10,21}

At 5 K, the shape of superconducting hysteresis loop with a large remanent molar magnetization M_r of $83 \text{ G cm}^3/\text{mol}$ indicates a strong pinning as well as a good indication of bulk nature of superconductivity for the oxygen-annealed sample. The remanent M_r decreases to $4 \text{ G cm}^3/\text{mol}$ at 30 K and $1 \text{ G cm}^3/\text{mol}$ at 35 K, where a weak-ferromagnetic background can be clearly seen. Fluctuation in the hysteresis loop is probably also related to the weak-ferromagnetic order.

To study the high-field effect on superconductivity, the magnetoresistivity $\rho(T, B_a)$ for $\text{RuSr}_2\text{GdCu}_2\text{O}_8$ up to 7 T are collectively shown in Fig. 5. The broadening of the resistive transition in magnetic fields is the common features for all high- T_c cuprate superconductors.⁴⁷ The normal-state resistivity is field independent and follows a T^2 dependence below T_c , with the superconducting $T_c(\text{onset})$ of 56 K in the zero field decreases slightly to 53 K in 7-T field. The temperature dependence of upper critical field $B_{c2}(T)$ can be fitted with a linear function $B_{c2}(0)[1 - T/T_c]$ with average $B_{c2}(0) = 133 \text{ T}$.⁴⁷ An average coherence length $\xi_0^{\text{ave}} = [\Phi_0/2\pi B_{c2}^{\text{ave}}(0)]^{1/2}$ of 0.5 nm with the Ginzburg-Landau

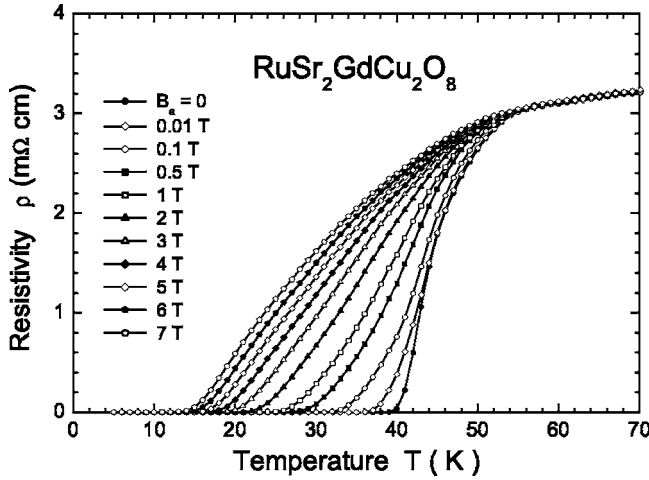


FIG. 5. Temperature dependence of magnetoresistivity $\rho(T, B_a)$ for $\text{RuSr}_2\text{GdCu}_2\text{O}_8$ in applied field up to 7 T.

parameter κ of 1040 and the thermodynamic critical field $B_c(0) = (B_{c1}B_{c2})^{1/2} = 0.32$ T. No anisotropic ξ_{ab} and ξ_c values can be estimated from present data. The $T_c(\text{zero})$ decreases from 39 K in zero applied field to 32 K in 1-kG, 28 K in 5-kG, 25 K in 1-T, 22 K in 2-T, 19 K in 3-T, 17 K in 4-T, 16 K in 5-T, 15 K in 6-T, and 14 K in 7-T field. If the zero resistivity is taken as the lower bound of the vortex melting temperature T_m , then the temperature dependence of the vortex melting transition line $B_m(T)$ can be fitted roughly by the formula $B_m(T) = B_m(0)[1 - T/T_m]^{3.5}$ with $B_m(0) = 35$ T and large exponent 3.5. In the lower field region, $B_m(T)$ rises as $[1 - T/T_m]^2$ as predicted by the mean-field approximation for temperature near $T_m = 39$ K.⁴⁷ The full phase diagram $B_a(T)$ of $\text{RuSr}_2\text{GdCu}_2\text{O}_8$ is shown in Fig. 6 to exhibit both the high- and low-field features. The very broad vortex liquid region with $\Delta T = 17$ K in zero field and $\Delta T = 42$ K in 7-T field is extraordinary and is most likely originated from the coexistence and the interplay between superconductivity and weak-ferromagnetic order. This magnetic order is so weak that superconductivity can coexist with the magnetic order, but the effect of a weak spontaneous magnetic moment $\mu_s \sim 0.1 \mu_B$ is detected through the appearance of a spontane-

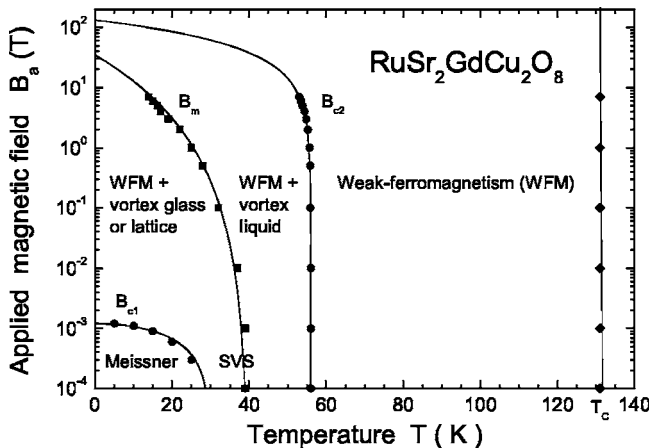


FIG. 6. Full phase diagram $B_a(T)$ of $\text{RuSr}_2\text{GdCu}_2\text{O}_8$.

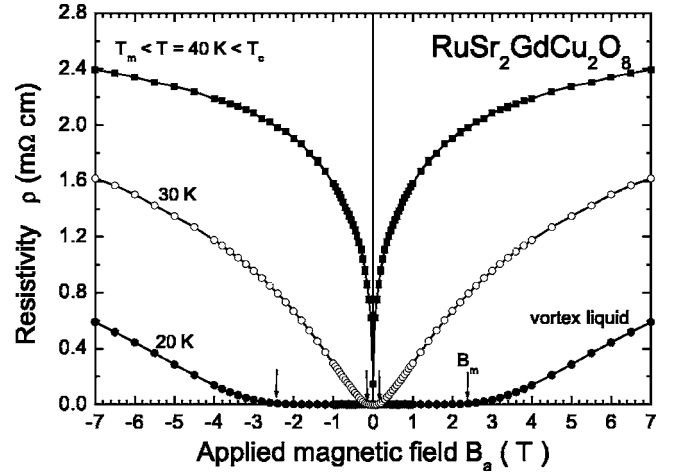


FIG. 7. Field dependence of magnetoresistivity $\rho(B_a)$ for $\text{RuSr}_2\text{GdCu}_2\text{O}_8$ in the vortex state at 20, 30, and 40 K. The zero resistivity gives a lower bound of vortex melting field B_m at 20 K.

ous vortex state above 30 K with a broad spontaneous vortex liquid region above T_m of 39 K.

To study the broad vortex liquid region, the isothermal field-dependent magnetoresistivity $\rho(B_a)$ for $T < T_c$ are shown in Fig. 7, where the zero resistivity gives a lower bound of the vortex melting field B_m . In the resistive vortex liquid region, the magnetoresistivity increases with increasing applied magnetic field and temperature. At 40 K, the magnetoresistivity is rapidly approaching a saturation value in an extrapolated saturation field $B_a \sim B_{c2}(40 \text{ K}) \sim 40$ T.

The last issue to be addressed is the depression of T_c by small spontaneous Ru magnetic moments. The weak-ferromagnetic order is actually a canted antiferromagnetic order that can coexist with superconductivity. However, the observed T_c of 56 K is too low as compared with 93 K for $\text{YBa}_2\text{Cu}_3\text{O}_7$ or 103 K for $\text{TlBa}_2\text{CaCu}_2\text{O}_7$. The depression of T_c by small spontaneous magnetic moment can be partially recovered by substitution of nonmagnetic Cu ions at Ru site. For example, in the $\text{Ru}_{1-x}\text{Cu}_x\text{Sr}_2\text{GdCu}_2\text{O}_8$ system, T_c onset up to 65 K for $x = 0.1$ and 72 K for $x = 0.4$ was reported.^{26,29}

IV. CONCLUSION

The lower critical field with $B_{c1}(0) = 12$ G and $T_0 = 30$ K indicates the existence of a spontaneous vortex state (SVS) between 30 K and T_c of 56 K. This SVS state is closely related with the weak-ferromagnetic order with a net spontaneous magnetic moment of $\sim 0.1 \mu_B$ per Ru. The broad vortex liquid region observed above vortex melting line $B_m(T)$ is also due to the coexistence and the interplay between superconductivity and weak-ferromagnetic order. Indeed, a possible spontaneous vortex state was also reported in the weak ferromagnetic superconductor Ru_{1222} compound $\text{RuSr}_2(\text{Eu}_{1.5}\text{Ce}_{0.5})\text{Cu}_2\text{O}_{10}$.⁴⁸

ACKNOWLEDGMENTS

This work was supported by the National Science Council of R.O.C. under Contract No. NSC93-2112-M007-011. We thank Dr. B. N. Lin for helpful discussions.

*Electronic address: hcku@phys.nthu.edu.tw

- ¹L. Bauernfeind, W. Widder, and H. F. Braun, *Physica C* **254**, 151 (1995).
- ²L. Bauernfeind, W. Widder, and H. F. Braun, *J. Low Temp. Phys.* **105**, 1605 (1996).
- ³K. B. Tang, Y. T. Qian, L. Yang, Y. D. Zhao, and Y. H. Zhang, *Physica C* **282-287**, 947 (1997).
- ⁴J. L. Tallon, C. Bernhard, M. Bowden, P. Gilberd, T. Stoto, and D. Pringle, *IEEE Trans. Appl. Supercond.* **9**, 1696 (1999).
- ⁵C. Bernhard, J. L. Tallon, Ch. Niedermayer, Th. Blasius, A. Golnik, E. Brucher, R. K. Kremer, D. R. Noakes, C. E. Stronach, and E. J. Ansaldo, *Phys. Rev. B* **59**, 14099 (1999).
- ⁶A. C. McLaughlin, W. Zhou, J. P. Attfield, A. N. Fitch, and J. L. Tallon, *Phys. Rev. B* **60**, 7512 (1999).
- ⁷J. L. Tallon, J. W. Loram, G. V. M. Williams, and C. Bernhard, *Phys. Rev. B* **61**, R6471 (2000).
- ⁸C. Bernhard, J. L. Tallon, E. Brucher, and R. K. Kremer, *Phys. Rev. B* **61**, R14960 (2000).
- ⁹J. W. Lynn, B. Keimer, C. Ulrich, C. Bernhard, and J. L. Tallon, *Phys. Rev. B* **61**, R14964 (2000).
- ¹⁰O. Chmaissem, J. D. Jorgensen, H. Shaked, P. Dollar, and J. L. Tallon, *Phys. Rev. B* **61**, 6401 (2000).
- ¹¹G. V. M. Williams and S. Kramer, *Phys. Rev. B* **62**, 4132 (2000).
- ¹²C. W. Chu, Y. Y. Xue, S. Tsui, J. Cmaidalka, A. K. Heilman, B. Lorenz, and R. L. Meng, *Physica C* **335**, 231 (2000).
- ¹³A. C. McLaughlin, V. Janowitz, J. A. McAllister, and J. P. Attfield, *Chem. Commun. (Cambridge)* **2000**, 1331 (2000).
- ¹⁴X. H. Chen, Z. Sun, K. Q. Wang, Y. M. Xiong, H. S. Yang, H. H. Wen, Y. M. Ni, and Z. X. Zhao, *J. Phys.: Condens. Matter* **12**, 10561 (2000).
- ¹⁵R. L. Meng, B. Lorenz, Y. S. Wang, J. Cmaidalka, Y. Y. Xue, and C. W. Chu, *Physica C* **353**, 195 (2001).
- ¹⁶V. P. S. Awana, J. Nakamura, M. Karppinen, H. Yamauchi, S. K. Malik, and W. B. Yelon, *Physica C* **357-360**, 121 (2001).
- ¹⁷D. P. Hai, S. Kamisawa, I. Kakeya, M. Furuyama, T. Mochiku, and K. Kadowaki, *Physica C* **357-360**, 406 (2001).
- ¹⁸A. P. Litvinchuk, S. Y. Chen, M. N. Iliev, C. L. Chen, C. W. Chu, and V. N. Popov, *Physica C* **361**, 234 (2001).
- ¹⁹C. T. Lin, B. Liang, C. Ulrich, C. Bernhard, *Physica C* **364-365**, 373 (2001).
- ²⁰H. Takagiwa, J. Akimitsu, H. Kawano-Furukawa, and H. Yoshizawa, *J. Phys. Soc. Jpn.* **70**, 333 (2001).
- ²¹J. D. Jorgensen, O. Chmaissem, H. Shaked, S. Short, P. W. Klamut, B. Dabrowski, and J. L. Tallon, *Phys. Rev. B* **63**, 054440 (2001).
- ²²R. S. Liu, L.-Y. Jang, H.-H. Hung, and J. L. Tallon, *Phys. Rev. B* **63**, 212507 (2001).
- ²³M. Pozek, A. Dulcic, D. Paar, G. V. M. Williams, and S. Kramer, *Phys. Rev. B* **64**, 064508 (2001).
- ²⁴V. G. Hadjiev, J. Backstrom, V. N. Popov, M. N. Iliev, R. L. Meng, Y. Y. Xue, and C. W. Chu, *Phys. Rev. B* **64**, 134304 (2001).
- ²⁵Y. Tokunaga and H. Kotegawa and K. Ishida and Y. Kitaoka and H. Takagiwa, and J. Akimitsu, *Phys. Rev. Lett.* **86**, 5767 (2001).
- ²⁶P. W. Klamut, B. Dabrowski, S. Kolesnik, M. Maxwell, and J. Mais, *Phys. Rev. B* **63**, 224512 (2001).
- ²⁷B. Lorenz, Y. Y. Xue, R. L. Meng, and C. W. Chu, *Phys. Rev. B* **65**, 174503 (2002).
- ²⁸T. P. Papageorgiou, H. F. Braun, and T. Herrmannsdorfer, *Phys. Rev. B* **66**, 104509 (2002).
- ²⁹H. Fujishiro, M. Ikebe, and T. Takahashi, *J. Low Temp. Phys.* **131**, 589 (2003).
- ³⁰C. Shaou, H. F. Braun, and T. P. Papageorgiou, *J. Alloys Compd.* **351**, 7 (2003).
- ³¹A. Vecchione, M. Gombos, C. Tedesco, A. Immirzi, L. Marchese, A. Frache, C. Noce, and S. Pace, *Int. J. Mod. Phys. B* **17**, 899 (2003).
- ³²F. Cordero, M. Ferretti, M. R. Cimberle, and R. Masini, *Phys. Rev. B* **67**, 144519 (2003).
- ³³H. Sakai, N. Osawa, K. Yoshimura, M. Fang, and K. Kosuge, *Phys. Rev. B* **67**, 184409 (2003).
- ³⁴Y. Y. Xue, F. Chen, J. Cmaidalka, R. L. Meng, and C. W. Chu, *Phys. Rev. B* **67**, 224511 (2003).
- ³⁵J. E. McCrone, J. L. Tallon, J. R. Cooper, A. C. MacLaughlin, J. P. Attfield, and C. Bernhard, *Phys. Rev. B* **68**, 064514 (2003).
- ³⁶A. Lopez, I. Souza Azevedo, J. E. Musa, E. Baggio-Saitovitch, and S. Garcia Garcia, *Phys. Rev. B* **68**, 134516 (2003).
- ³⁷S. Garcia, J. E. Musa, R. S. Freitas, and L. Ghivelder, *Phys. Rev. B* **68**, 144512 (2003).
- ³⁸T. P. Papageorgiou, H. F. Braun, T. Gorlach, M. Uhlarz, and H. v. Lohneysen, *Phys. Rev. B* **68**, 144518 (2003).
- ³⁹P. W. Klamut, B. Dabrowski, S. M. Mini, M. Maxwell, J. Mais, I. Felner, U. Asaf, F. Ritter, A. Shengelaya, R. Khasanov, I. M. Savic, H. Keller, A. Wisniewski, R. Puzniak, I. M. Fita, C. Sulkowski, and M. Matusiak, *Physica C* **387**, 33 (2003).
- ⁴⁰T. Nachtrab, D. Koelle, R. Kleiner, C. Bernhard, and C. T. Lin, *Phys. Rev. Lett.* **92**, 117001 (2004).
- ⁴¹Y. Y. Xue, B. Lorenz, A. Baikalov, J. Cmaidaka, F. Chen, R. L. Meng, and C. W. Chu, *Physica C* **408-410**, 638 (2004).
- ⁴²S. Garcia and L. Ghivelder, *Phys. Rev. B* **70**, 052503 (2004).
- ⁴³C. J. Liu., C. S. Sheu, T. W. Wu, L. C. Huang, F. H. Hsu, H. D. Yang, G. V. M. Williams, and Chia-Jung C. Liu, *Phys. Rev. B* **71**, 014502 (2005).
- ⁴⁴Y. C. Lin, T. Y. Chiu, M. F. Tai, B. N. Lin, P. C. Guan, and H. C. Ku, *Int. J. Mod. Phys. B* **19**, 339 (2005).
- ⁴⁵T. Y. Chiu, Y. C. Lin, M. F. Tai, B. N. Lin, P. C. Guan, B. C. Chang, and H. C. Ku, *Chin. J. Phys. (Taipei)* **43**, 616 (2005).
- ⁴⁶H. C. Ku, C. Y. Yang, B. C. Chang, B. N. Lin, Y. Y. Hsu, and M. F. Tai, *J. Appl. Phys.* **97**, 10B110 (2005).
- ⁴⁷M. Tinkham, *Introduction to Superconductivity* (McGraw-Hill, Inc. Singapore, 1996), Chap. 9. 2nd ed.
- ⁴⁸B. D. Hennings, K. D. D. Rathnayaka, D. G. Naugle, and I. Felner, *Physica C* **370**, 253 (2002).